

文章编号: 1007 - 1482(2006)03 - 0157 - 06

· 论著 ·

Determination of dislocation boundary spacings from length per area measurements in EBSD data sets

YANG Jing, GODFREY Andrew, YU Tianbo, LIU Qing

(Laboratory of Advanced Material of Dept Materials Science and Engineering,
Tsinghua University, Beijing 100084, P. R. China)

Abstract: In this paper we examine the effect on the determination of boundary length per unit area of the stepped nature of boundaries in orientation maps derived from electron back-scatter diffraction data. A correction factor is derived for isotropic microstructures. Two measures based on length per unit area for the determination of the cross-link boundary spacing in high strain deformation microstructures are then compared. A geometric method based on subtraction of the contribution to the length per area of the lamellar boundaries gives the best results, though in some cases a method based on boundary misorientation angles may be preferred.

Key words: deformation microstructure; EBSD/EBSP; dislocation boundary

It is well established now that for many metals a fraction of the dislocations introduced during plastic deformation remain in the material after deformation, and are arranged into dislocation boundaries^[1-3]. These dislocation boundaries are in fact rotation boundaries, separating volumes of material with different crystallographic orientations^[2-4]. An important parameter characterizing each dislocation boundary is therefore the misorientation angle across the boundary. Another important parameter required for quantitative characterization of dislocation boundary microstructures formed during plastic deformation is the spacing between the boundaries. Both the average boundary spacing and the average misorientation angle vary both with strain as well as with deformation mode^[4-6]. A quantitative characterization of these boundaries is important for many problems, including mechanical strength^[6,7], stored energy^[8], and annealing behavior^[9,10].

Traditionally measurements of spacing and misorientation angle have been carried out in the transmission electron microscope^[11,12]. As an alternative the electron back-scatter pattern diffraction (EBSD) technique can also be used to obtain such data. However, the

EBSD technique suffers from a worse angular and spatial resolution than in the Transmission Electron Microscope (TEM)^[13,14]. A further problem is that TEM investigations have shown that dislocation boundaries can be divided into two classes, namely extended planar boundaries (sometimes referred to as geometrically necessary boundaries, GNBs) and shorter incidental dislocation boundaries (DBs)^[12-6]. For example, after rolling to high strains (>1.5) the GNBs tend to lie as sheets parallel to the rolling plane, with the DBs cross-linking between these sheets^[15]. These two boundary classes are generated by different mechanisms and show a different evolution with strain. For many applications it is very useful to be able to separate the boundaries within a given microstructure into these two classes.

Quantitative information concerning boundary spacings can be obtained from EBSD data by line-intercept measurements (such a feature is supplied in all the commercially available EBSD post-processing software). However, in certain cases line-intercept measurements may not give a reasonable sampling of the microstructure. Area-based measurements ("grain recon-

Accepted date: 2006 - 05 - 23

Supported by the National Natural Science Foundation of China (No. 50371041 and No. 50571049)

corresponding author: awgodfrey@mails.tsinghua.edu.cn

struction”) can also be used, but these methods suffer from other problems, particularly when applied to deformed microstructures^[14]. As an EBSD data is usually presented in the form of an orientation map each data set in fact contains directly information about the length per unit area (L_A) of boundaries in the microstructure. An important problem, however, with obtaining data for L_A from an EBSD data set is that the boundaries in an EBSD orientation map are stepped in nature, as a result of the underlying mapping grid. In this paper we consider the effect of this stepped boundary nature on measurements of L_A and then compare two different techniques, both based on L_A measurements, for determining the average spacing of the cross-linking boundaries in high strain deformation microstructures.

1 Effect of stepped boundaries on measurement of L_A

The length per area of boundary with misorientation angle more than θ^* can be determined from

$$L_{A,EBSD}(\theta > \theta^*) = N(\theta > \theta^*) / A$$
$$= N(\theta > \theta^*) / A, \tag{1}$$

where $N(\theta > \theta^*)$ is the number of misorientations greater than θ^* , Δ is the map step size, and A is the map area (in pixels²). All these numbers are available directly from the standard post-processing software packages. The problem arising from the stepped nature of boundaries in an EBSD map is shown in Fig 1. Here the real length of the boundary is $L_{true} = AC$. However this boundary is represented in the EBSD map as a series of horizontal and vertical lines (in this study we consider only a square mapping grid; the analysis can also be extended to include a hexagonal mapping grid) so that the apparent length of the boundary is now $L_{EBSD} = AB + BC$, resulting in an overestimate of the true value, i.e. $L_{EBSD} > L_{true}$. It is clear that the amount of this overestimate depends on the angle α ; for $\alpha = 0^\circ$ (or 90°) $\cos \alpha = 1$, whereas the maximum error ($\cos \alpha = 0$) is for $\alpha = 45^\circ$. In general for an EBSD map the overestimate (ϵ) will depend on the distribution of boundary angles $P(\alpha)$. Assuming that α is uniformly distributed and that there is no correlation between the length of each boundary and the angle α , we can calculate a correction factor as follows

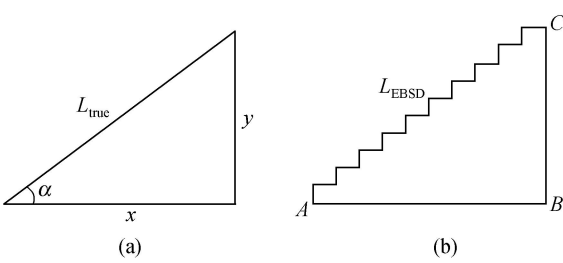


Fig 1 Illustration of the geometry of the boundary step problem in EBSD maps: (a) real boundary; (b) representation of this boundary in a square-grid EBSD map

From Fig 1b we note that $L_{EBSD} = x + y = x(1 + \tan \alpha)$ and that $L_{true} = x / \cos \alpha$. Eliminating x we have

$$L_{EBSD} = L_{true} \cos \alpha (1 + \tan \alpha), \tag{2}$$

$$\text{so that } \epsilon = L_{EBSD} / L_{true} = \cos \alpha (1 + \tan \alpha)$$
$$= \cos \alpha + \sin \alpha. \tag{3}$$

The value of ϵ^* is then obtained by integrating this expression over the appropriate angular range (in this case from 0° to $45^\circ = \pi/4$) using the relationship^[16]

$$\overline{f(\alpha)} = \frac{1}{\int_0^{\pi/4} \cos^2 \alpha - \sin^2 \alpha \, d\alpha} \int_0^{\pi/4} f(\alpha) \, d\alpha, \tag{4}$$

i.e.,

$$\epsilon^* = \frac{1}{\int_0^{\pi/4} (\cos^2 \alpha - \sin^2 \alpha) \, d\alpha} \int_0^{\pi/4} (\cos \alpha + \sin \alpha) \, d\alpha$$
$$= \frac{4}{\pi} \int_0^{\pi/4} (\sin \alpha - \cos \alpha) \, d\alpha$$
$$= 4/\pi. \tag{5}$$

The validity of this relationship is tested using an EBSD map of a fully recrystallized sample of AA1090 (Fig 2). For this map the value of $N_L(\theta > 2^\circ)$, as determined from the average of two perpendicular sets of test lines is $0.051 \mu\text{m}^{-1}$. This can be converted to a length per area following the standard equivalence

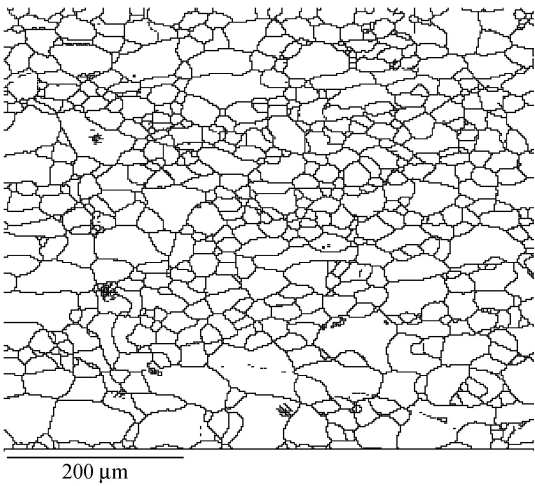


Fig 2 Example EBSD orientation map for a fully recrystallized sample of AA1090. The map shows all misorientations with angle $> 2^\circ$

$$L_A = (\sqrt{2}) N_L \tag{6}$$

giving a value of $L_A = 0.081 \mu\text{m}^{-1}$. The length per area calculated directly from the EBSD data according to Eqn (1) is $0.105 \mu\text{m}^{-1}$. The difference between these two values is 1.29, which is very close to the predicted required correction factor of $4 / (1.273)$. It is worthwhile noting that the value obtained from an area measurement is considerably higher. This is because area-based measurements are strongly affected by the presence in the data of artificial grains consisting of just 1 or 2 pixels. Note that in this analysis we have assumed boundary curvature can be ignored by approximating each boundary segment as a straight line. In practice there will also be some error associated with this assumption, but this error can be minimized by taking the step-size as a small fraction of the average curvature.

2 Determining the spacing of cross-linking boundaries at high strains

In this next section we consider how to determine from length per area data the average spacing of the cross-linking boundaries in deformation microstructures of samples rolled to high plastic strains. An idealized sketch of such a microstructure is shown in Fig 3. Note that the cross-linking boundaries can be either perpendicular, or may take a range of angles, to the lamellar boundaries. Determination of the lamellar boundary spacing from line scans placed perpendicular to these boundaries can be carried out using the standard post-processing software. It is more difficult however to obtain the average spacing of the cross-linking boundaries as (1) the lamellar boundaries are usually somewhat wavy in nature, and (2) intercept data from test lines must be taken manually, and not in an automated fashion, by carefully placing the test-lines between the lamellar boundaries. It is possible however to obtain an estimate of the spacing of the cross-linking boundaries from the length per area data, and two methods for doing this are presented in the following.

The first method is geometric in nature. We note that the lamellar spacing can be determined easily from perpendicular line scans as $d_{\text{lam}}(4^\circ)$ (here we assume that the lamellar boundaries have misorientations $>4^\circ$,

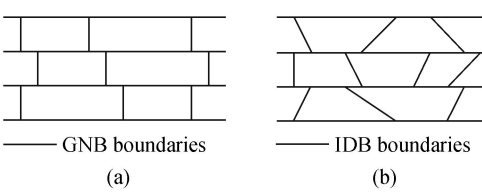


Fig 3 Sketch showing idealized lamellar microstructure with the cross-linking boundaries (a) perpendicular and (b) lying at a range of angles, to the lamellar boundaries

as observed in TEM studies^[15]). The length per area for these boundaries is simply given by $L_{A, \text{lam}}(4^\circ) = 1 / d_{\text{lam}}(4^\circ)$. The length per area of the cross-linking boundaries ($L_{A, \text{cl}}$) is then given by

$$L_{A, \text{cl}}(G) = L_{A, \text{EBSD}}(\theta^*) - L_{A, \text{lam}}(4^\circ), \tag{7}$$

where the total length per area is taken using a minimum misorientation definition of θ^* , ideally as low as possible, but in practice a value of 2° is typically used for heavily deformed metals.

The second method for obtaining the length per area of these cross-linking boundaries relies on the assumption that the majority of these boundaries are of the DB type. Even in very highly deformed samples the average DB angle does not exceed 4° , so that an approximate separation of the DBs can be made by selecting only those boundaries with misorientation angles of less than 4° . Again the limited angular resolution of the EBSD technique requires that we also define a lower limit of $\theta^* = 2^\circ$. In this case the length per area of the cross-linking boundaries can be written as

$$L_{A, \text{cl}}(A) = L_{A, \theta^* < 4^\circ} \\ = L_{A, \text{EBSD}}(\theta^*) - L_{A, \theta^* > 4^\circ}, \tag{8}$$

In both cases in order to convert from a length per area value to an average spacing we need to make an assumption as to whether or not the cross-linking boundaries are perpendicular to the lamellar boundaries. In the former case we do not need to correct for boundary steps (for the lamellar boundaries $\theta = 0^\circ$ and for the cross-linking boundaries $\theta = 90^\circ$, so that $d_{\text{cl}} = 1 / L_{A, \text{cl}}$ (geometric method). If, however, the cross-linking boundaries lie with a range of angles to the lamellar boundaries, it is necessary to apply the correction factor (θ^*) discussed in section 2. In this case

$$d_{\text{cl}} = (\sqrt{2}) (\theta^* / L_{A, \text{cl}}). \tag{9}$$

Both the geometric and misorientation angle methods (Eqns 7 and 8, respectively) are compared using

data for AA1100 deformed by the accumulated roll-bonding process^[17] up to a strain of $\epsilon_M = 4.8$. An example EBSD orientation map for a sample deformed by the ARB process to a strain of $\epsilon_M = 2.4$ is shown in Fig 4. Note that in this figure the white regions are areas where indexing was not possible. The area of these regions was excluded when calculating the value of length per area (i.e., map area = total map area \times fraction indexed). The results are summarized in Table 1. For the calculation of d_{cl} we assume that the cross-linking boundaries can take a range of angle to the lamellar boundaries. The geometric method gives a consistently lower value for the spacing than the misorientation angle method. This is understandable since in practice, particularly for the ARB technique, a significant fraction of the cross-linking boundaries have misorientation angle greater than 4° . It should be noted that even the d_{cl} (G) value is slightly higher than the

reported spacing from TEM investigations, presumably due to the fact that cross-linking boundaries with misorientation angles less than 2° have not been identified at present (due to the angular resolution limitation of the technique).

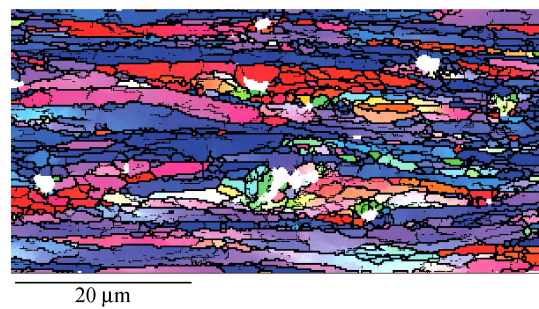


Fig 4 Example EBSD orientation map for a sample of AA1100 deformed to a strain of $\epsilon_M = 2.4$ by the ARB process. Misorientations of $>2^\circ$ and $>4^\circ$ are shown in thin and thick black lines respectively. The color represents the crystal direction parallel to the normal direction in the rolling coordinate system.

Table 1 Calculations of d_{cl} (geometric) and d_{cl} (Angle)

ϵ_M	d_{lam} (μm)	$L_{A, tot}$ (μm^{-1})	$L_{A, lam}$ (μm^{-1})	$L_{A, >4^\circ}$ (μm^{-1})	$L_{A, cl}$ (G) (μm^{-1})	$L_{A, cl}$ (A) (μm^{-1})	d_{cl} (G) (μm)	d_{cl} (A) (μm)
2.4	0.47	3.98	2.14	3.02	1.81	0.96	1.09	2.08
4.0	0.36	4.68	2.87	4.11	1.84	0.57	1.11	3.49
4.8	0.29	7.52	3.44	5.85	4.08	1.66	0.49	1.20

Notes: $L_{A, cl}$ (G): calculated using geometric method (Eqn. 7)
 $L_{A, cl}$ (A): calculated using misorientation angle method (Eqn. 8)

3 Discussion

One reason for the difference in the two methods is that not all of the cross-linking boundaries are of low misorientation angle. The fraction of cross-linking boundaries with misorientation angles greater than 4° will be expected to increase with strain, and this is reflected in ratio of d_{cl} (A) / d_{cl} (G) (Fig 5). Another problem with the misorientation angle method is that the threshold angle used to separate the GNBs from the DBs should really be chosen as a function of strain (as well as the material and the deformation mode). For example, in a TEM study of cold-rolled nickel the average misorientation angle across boundaries identified as DBs increased from 0.9° at a strain $\epsilon_M = 0.26$ to 3.0° at a strain $\epsilon_M = 4.5$ ^[15]. A problem common to both methods is the requirement of setting a lower threshold on the misorientation

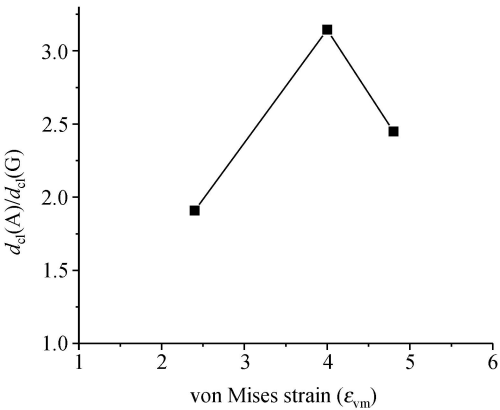


Fig 5 Graph showing the ratio between d (geometric) and d (angle) as a function of strain for the ARB data.

to define a dislocation boundary. This lower threshold is needed to avoid distortions to the data due to “orientation noise” (spurious misorientations arising as a result of the limited angular resolution). In the current study we have used a lower threshold of 2° . It is expected however that there will be a certain number of DBs

with misorientation angles below this value. In some cases advanced orientation filtering methods can allow the use of a lower misorientation angle threshold, but such techniques are as yet untested on such highly strained microstructures.

The choice of method for estimation of the cross-link boundary spacing will depend mostly on the intended use of the data. For example, for calculations relating the yield strength to the microstructure it is usual to define a boundary misorientation above which the boundary acts as a grain boundary, and below which it acts as a dislocation boundary^[18]. For such calculations the misorientation angle method is obviously more appropriate. For input to models of microstructure evolution during annealing it is more important to know the dislocation cell size. In such a case the geometric method will be preferred as this method gives a figure representing the average spacing between all the cross-linking boundaries. In both cases it is necessary make a correction for the stepped nature of the boundaries, to avoid an overestimation of the length per unit area.

4 Conclusion

Quantitative information about the length per area data of boundaries can be obtained directly from an EBSD orientation map. However, the stepped nature of boundaries in EBSD orientation maps requires a correction for the use of such data. A correction factor can be calculated based on an assumption concerning the spatial arrangement of the boundaries in the microstructure. The measure of length per area is particularly useful for the determination of the boundary spacing of the cross-linking boundaries in high strain lamellar deformation microstructures developed by rolling. Two methods have been proposed for the estimation of the cross-link boundary spacing. The choice of method will largely depend upon the final use of the data. In both cases it should be remembered that the limited angular resolution of the EBSD technique prevents detection of boundaries below a certain minimum misorientation threshold. The methods described in this paper will be applicable to data sets taken with a better angular resolution, if and when such techniques become available.

Acknowledgements

This project was supported by the National Natural Science Foundation of China under contract numbers 50371041 and 50571049.

References:

- [1] Bay B, Hansen N, Kuhmann-Wilsdorf D. Microstructural Evolution in Rolled Aluminium [J]. *Materials Science and Engineering*, 1992, A158: 139 - 146.
- [2] Liu Q, Juul Jensen D and Hansen N. Effect of Grain Orientation on Deformation Structure in Cold-rolled Polycrystalline Aluminium [J]. *Acta mater*, 1998, 46: 5819 - 5838.
- [3] Hansen N and Huang X. Microstructure and Flow Stress of Polycrystals and Single Crystals [J]. *Acta mater*, 1998, 46: 1827 - 1836.
- [4] Hansen N and Juul Jensen D. Development of Microstructure in FCC Metals during Cold Work [J]. *Proc of the Royal Society*, 1999, 357: 1447 - 1469.
- [5] Pantleon W, Hansen N. Disorientations in Dislocation Boundaries: Formation and Spatial Correlation [J]. *Materials Science and Engineering*, 2001, A309-310: 246 - 250.
- [6] Li BL, Godfrey A, Meng QC, Liu Q, Hansen N. Microstructure Evolution of IF-steel During Cold Rolling [J]. *Acta mater*, 2004, 52: 1069 - 1081.
- [7] Nes E, Marthinsen K, and Homedal B. The Effect of Boundary Spacing on Substructure Strengthening [J]. *Materials Science and Technology*, 2004, 20: 1377 - 1382.
- [8] Godfrey A, Cao WQ, Hansen N and Liu Q. Stored Energy, Microstructure, and Flow Stress of Deformed Metals [J]. *Metallurgical and Materials Transactions A*, 2005, 36A: 2371 - 2378.
- [9] Prangnell PB, Hayes JS, Bowen JR, Apps PJ, and Bate PS. Continuous recrystallisation of lamellar deformation structures produced by severe deformation [J]. *Acta mater*, 2004, 52: 3193 - 206.
- [10] Jazaeri H and Humphreys FJ. The Transition from Discontinuous to Continuous Recrystallization in Some Aluminium Alloys: II—Annealing Behaviour [J]. *Acta Materialia*, 2004, 52: 3251 - 3262.
- [11] Liu Q. A Simple Method for Determining Orientation and Misorientation of the Cubic Crystal Specimen [J]. *Appl Cryst*, 1994, 27: 755 - 761.

[12] Liu Q, Hansen N. Geometrically Necessary Boundary and Incidental Dislocation Boundary Formed during Cold Deformation [J]. *Scr Metall Mater*, 1995, 32 (8): 1289 - 1295.

[13] Humphreys F J, Huang Y, Brough I , Harris C. Electron Backscatter Diffraction of Grain and Subgrain Structures—Resolution Considerations [J]. *J Microsc*, 1999, 195 (3): 212 - 216.

[14] Mishin OV, Godfrey A. and Ostensson L. Comparative Microstructural Characterization of a Friction-Stir-Welded Aluminum Alloy Using TEM and SEM-Based Techniques [J]. *Metallurgical and Materials Transactions A*, 2006, 37A: 489 - 496.

[15] Hughes D A, Hansen N. Microstructure and Strength of Nickel at Large Strains [J]. *Acta mater*, 2000, 48 (11): 2985 - 3004.

[16] Rhines FN and DeHoff RT. Quantitative Microscopy [M]. *New York: McGraw-Hill*, 1968 ch. 3.

[17] Saito Y, Utsunomiya H, Tsuji N and Sakai T. Novel Ultra-high Straining Process for Bulk Materials—Development of the Accumulative Roll-Bonding (ARB) Process [J]. *Acta Mater*, 1999, 47 (2): 579 - 583.

[18] Hansen N. Boundary Strengthening in Undeformed and Deformed Polycrystals [J]. *Mater Sci Eng*, 2005, A409: 39 - 45.

· 动态与信息 ·

第 12 届国际体视学大会即将于 2007 年 9 月在法国召开

国际体视学大会 (ICS, 即 International Congress for Stereology) 是国际体视学学会 (ISS, 即 International Society for Stereology) 的重要活动之一, 每四年举行一次。

继在哥本哈根 (1995)、墨尔本 (1999)、圣地亚哥 (2003) 的前几届国际体视学大会以及第 11 届国际体视学大会北京卫星会议 (2003) 的成功举办, 第 12 届国际体视学大会 (ICS XII) 将于 2007 年 8 月 30 日至 9 月 7 日在法国的 Saint-Etienne 市召开。欢迎中国体视学学会会员及中国科技工作者积极与会。若必要, 中国体视学学会可考虑组团前往。欲参加者, 请在与会议承办人联系的同时, 与中国体视学学会联系。

会议由 Professor Michel JOURLIN 具体承办组织。
联系用电子邮箱: flora_jourlin@univ-st-etienne.fr
详情请询如下网址: <http://ICSXII.univ-st-etienne.fr/>